

## Virtual Screening Identification of Nonfolate Compounds, Including a CNS Drug, as Antiparasitic Agents Inhibiting Pteridine Reductase

Stefania Ferrari,<sup>†</sup> Federica Morandi,<sup>†,||</sup> Domantas Motiejunas,<sup>†,⊥</sup> Erika Nerini,<sup>†,‡</sup> Stefan Henrich,<sup>‡</sup> Rosaria Luciani,<sup>†</sup> Alberto Venturilli,<sup>†</sup> Sandra Lazzari,<sup>†</sup> Samuele Calò,<sup>†</sup> Shreedhara Gupta,<sup>§</sup> Veronique Hannaert,<sup>§</sup> Paul A. M. Michels,<sup>§</sup> Rebecca C. Wade,<sup>\*,‡</sup> and M. Paola Costi<sup>\*,†</sup>

<sup>†</sup>Dipartimento di Scienze Farmaceutiche, Università degli Studi di Modena e Reggio Emilia, Via Campi 183, 41100 Modena, Italy,

<sup>‡</sup>Heidelberg Institute for Theoretical Studies (HITS) gGmbH, Schloss-Wolfsbrunnweg 35, 69118 Heidelberg, Germany, and

<sup>§</sup>Research Unit for Tropical Diseases, de Duve Institute and Laboratory of Biochemistry, Université catholique de Louvain, Avenue Hippocrate 74, B-1200 Brussels, Belgium. <sup>||</sup>Current address: Merck Serono Switzerland. <sup>⊥</sup>Current address: CropDesign N.V., Technologiepark 3, B-9052 Gent, Belgium.

Received August 14, 2010

Folate analogue inhibitors of *Leishmania major* pteridine reductase (PTR1) are potential antiparasitic drug candidates for combined therapy with dihydrofolate reductase (DHFR) inhibitors. To identify new molecules with specificity for PTR1, we carried out a virtual screening of the Available Chemicals Directory (ACD) database to select compounds that could interact with *L. major* PTR1 but not with human DHFR. Through two rounds of drug discovery, we successfully identified eighteen drug-like molecules with low micromolar affinities and high in vitro specificity profiles. Their efficacy against *Leishmania* species was studied in cultured cells of the promastigote stage, using the compounds both alone and in combination with **1** (pyrimethamine; 5-(4-chlorophenyl)-6-ethylpyrimidine-2,4-diamine). Six compounds showed efficacy only in combination. In toxicity tests against human fibroblasts, several compounds showed low toxicity. One compound, **5c** (riluzole; 6-(trifluoromethoxy)-1,3-benzothiazol-2-ylamine), a known drug approved for CNS pathologies, was active in combination and is suitable for early preclinical evaluation of its potential for label extension as a PTR1 inhibitor and antiparasitic drug candidate.

### Introduction

Parasites of the Trypanosomatidae family are the causal agents of a number of serious human diseases, including African sleeping sickness, Chagas' disease, and leishmaniasis. The impact of these parasites on public health and the inadequacy of current treatments have created an urgent requirement for more effective drugs, since those in use are highly toxic and often difficult to administer. The problem is compounded by a rise in drug resistance. Therapy for leishmaniasis generally relies on old drugs such as sodium stibogluconate and Amphotericin B, and only one new treatment has been developed in the last 25 years, Miltefosine, which is approved in India for visceral Leishmaniasis.<sup>1</sup>

Enzymes involved in the provision of reduced folate cofactors, e.g., dihydrofolate reductase (DHFR<sup>a</sup>), and enzymes that utilize these cofactors, like thymidylate synthase (TS), are important drug targets for the treatment of bacterial infections,<sup>2</sup> cancer,<sup>3</sup> and certain parasitic diseases, notably malaria.<sup>4</sup> Inhibition of DHFR or TS leads to a reduction in the cellular pools of 2'-deoxythymidine-5'-monophosphate, severely impairs DNA replication, and results in cell death.

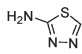
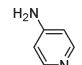
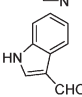
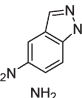
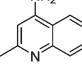
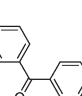
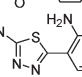
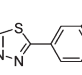
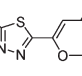
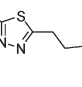
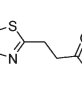
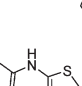
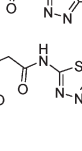
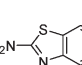
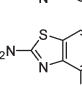
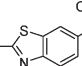
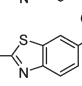
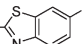
Trypanosomatids are auxotrophic for folates and pterins, and inhibition of the enzymes involved in the salvage pathways should provide effective treatment.<sup>5</sup> However, antifolates are currently not employed in therapy of trypanosomatid infections, mainly because of the pteridine reductase (PTR1) activity of the target organisms. PTR1 is a short-chain dehydrogenase/reductase that is able to carry out successive reductions of both conjugated (folate) and unconjugated (biopterin) pterins.<sup>6,7</sup> While the bifunctional DHFR-TS used by trypanosomatids can only reduce folic acid, PTR1 can act on a broader range of substrates. Under physiological conditions, PTR1 is responsible for the reduction of 10% of the folic acid required by the cell, but when classical antifolate drugs inhibit DHFR-TS, PTR1 can be overexpressed, ensuring parasite survival.<sup>8,9</sup> This suggests that treatment of trypanosomatid infections could be achieved through the simultaneous inhibition of DHFR and PTR1 by a single drug or a combination of compounds that are specific and selective inhibitors of both targets.<sup>8</sup>

Previous work in our laboratories<sup>10</sup> has demonstrated that it is possible to identify specific inhibitors of PTR1 and to use such inhibitors in combination with known antifolates to effectively improve in vitro efficacy against *Leishmania* and *Trypanosoma* species.<sup>10</sup> A similar approach has been taken to discover new compounds with pyrrolo[2,3-*d*]pyrimidine structures that are active against *Trypanosoma brucei* PTR1 and on bloodstream parasites.<sup>11</sup> Very recently, a virtual screening strategy revealed compounds with aminobenzothiazole and

\*To whom correspondence should be addressed. For M.P.C.: Phone 0039-059-205-5134; E-mail mariapaola.costi@unimore.it. For R.C.W.: Phone 0049-6221-533-247; E-mail rebecca.wade@h-its.org.

<sup>a</sup>Abbreviations: ACD, Available Chemicals Directory; DHFR, dihydrofolate reductase; PTR1, pteridine reductase; rmsd, root-mean-square deviation; TS, thymidylate synthase.

**Table 1.** Compounds with Inhibitory Activity against LmPTR1 and Their Biological Activity Profiles

Code	Structure	LmPTR1 IC <sub>50</sub> (μM) [Ki (μM)]	LmDHFR IC <sub>50</sub> (μM)	hDHFR IC <sub>50</sub> (μM)
4a		5600 [436]	NI <sup>a</sup>	NI <sup>b</sup>
6a		1900	NI <sup>a</sup>	NI <sup>a</sup>
28a		1100	2000 <sup>a</sup>	NI <sup>a</sup>
35a		1000	NI <sup>c</sup>	NI <sup>d</sup>
38a		390	NI <sup>a</sup>	NI <sup>a</sup>
53a		2300	NI <sup>c</sup>	NI <sup>c</sup>
7b		31 [2]	NI <sup>c</sup>	NI <sup>c</sup>
14b		309 [24]	NI <sup>c</sup>	NI <sup>c</sup>
15b		22 [2]	1300	NI <sup>c</sup>
21b		29 [2]	139 <sup>c</sup>	300
22b		89 [7]	NI <sup>c</sup>	NI <sup>c</sup>
28b		93 [7]	NI <sup>c</sup>	NI <sup>a</sup>
29b		116 [9]	NI <sup>c</sup>	NI <sup>ca</sup>
1c		1800 [143]	NI <sup>a</sup>	NI <sup>a</sup>
2c		1000 [79]	1390 <sup>a</sup>	NI <sup>a</sup>
3c		40 [3]	NI <sup>c</sup>	89 <sup>c</sup>
4c		212 [16]	1780 <sup>a</sup>	1040 <sup>a</sup>
5c		50 [4]	NI <sup>b</sup>	312 <sup>b</sup>

<sup>a-e</sup> NI: No inhibition. Measurements made with the following concentrations of compound: <sup>a</sup> 500 μM; <sup>b</sup> 1 mM; <sup>c</sup> 50 μM; <sup>d</sup> 100 μM; <sup>e</sup> 25 μM (see Materials and Methods).

aminobenzimidazole scaffolds that inhibit *Trypanosoma brucei* PTR1.<sup>12</sup> In the present paper, we describe the application of a different virtual screening approach combined with rapid synthetic and experimental screening methodologies that has enabled us to identify nonfolate like inhibitors of *Leishmania* PTR1 with thiazole core structures. The hits identified

have been optimized in two structure-based design cycles, including species specificity studies. The compounds were tested against the *Leishmania major* enzymes, LmPTR1 and LmDHFR-TS, and the human DHFR (hDHFR). The best compounds were also assayed against in vitro cultured cells of different trypanosomatid species, such as promastigotes of

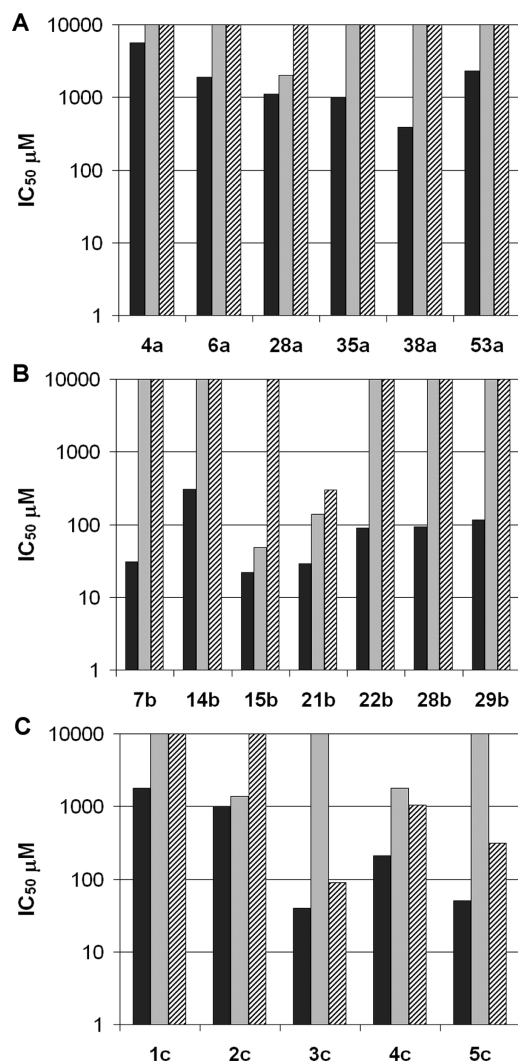


**Figure 1.** Inhibitory activity (IC<sub>50</sub> values) and specificity profile of (A) compounds from virtual screening, (B) derivatives from the thiadiazole library, and (C) benzothiazole compounds. The Y axis is on a logarithmic scale. The color code is as follows: LmPTR1, black; LmDHFR, gray; hDHFR, striped.

*L. mexicana* and *L. major*, both as single agents and in combination with **1** (pyrimethamine; 5-(4-chlorophenyl)-6-ethylpyrimidine-2,4-diamine)<sup>13</sup> (Supporting Information Figure 1-SI). The toxicity of these compounds was tested against human fibroblasts (MRC5).

## Results and Discussion

**Virtual Screening Hits and Scaffold Identification.** Virtual screening of the Available Chemicals Directory (ACD) database against the three-dimensional structure of LmPTR1 (PDB ID: 1E92) using the program LUDI<sup>14</sup> resulted in 21 394 docked molecules. Analysis of the available crystallographic structures showed that the substrate, dihydrobiopterin binds to LmPTR1 by forming an extended network of hydrogen bonds and aromatic stacking interactions with the cofactor and Phe113. During the selection of the docked molecules, we wanted to select compounds able to mimic the binding mode of this substrate. The docked molecules were initially filtered based on three calculated parameters: (I) the ability of the ligand to bind deep into the active site (contact percentage > 50); (II) the ability to replace the substrate by

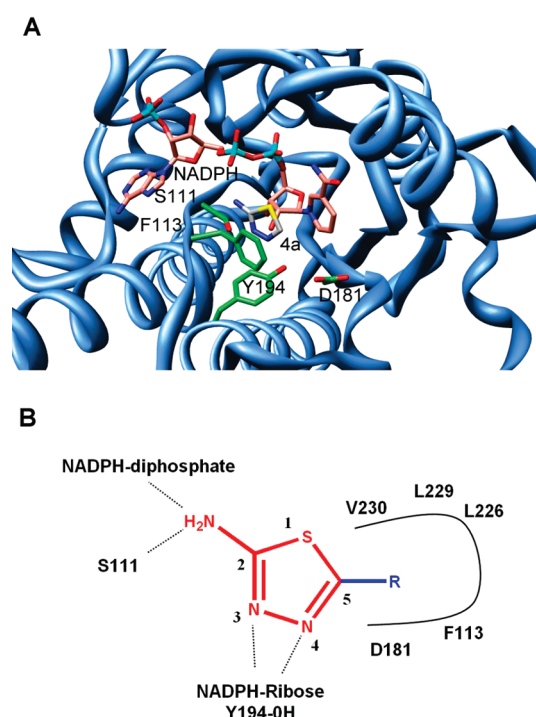
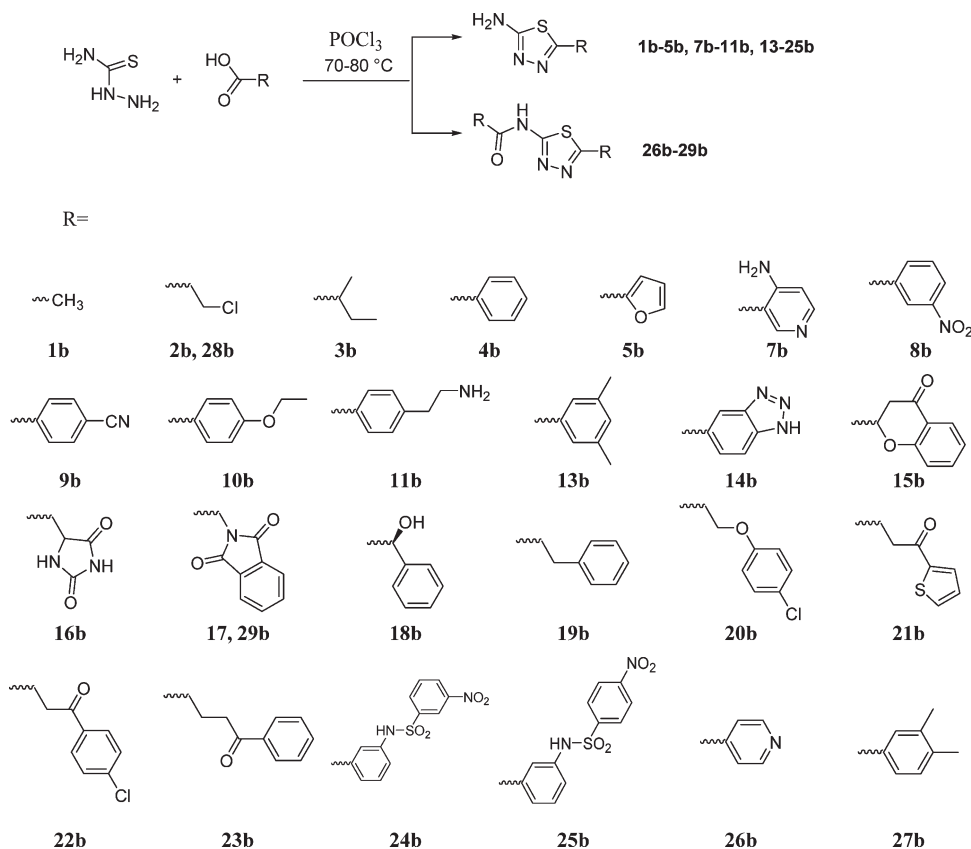


**Figure 2.** (A) Structure of LmPTR1 with compound **4a** bound as calculated with the LUDI software. (B) Schematic representation of the binding mode of compound **4a** derivatives with substituents at position 5.

forming hydrogen bonds with the active site residues (number of H bonds > 1); (III) the calculated score (> 400). The remaining 724 docking results were analyzed visually and molecules were selected based on (I) the number and type of interactions established, (II) which residues they interact with, and (III) comparison of the structures of the active sites of LmPTR1 and hDHFR. Molecules that were predicted to form a stacking interaction with Phe113 and to interact with LmPTR1 residues that are not conserved in the hDHFR active site were selected preferentially. This second selection resulted in 53 molecules that were purchased and tested against LmPTR1 (Supporting Information Table 1-SI). Six of these compounds (**4a**, **6a**, **28a**, **35a**, **38a**, **53a**) were found to be active against LmPTR1 with IC<sub>50</sub> values between 0.39 and 5.6 mM (Table 1, Figure 1). These molecules were further tested for their inhibitory activity against LmDHFR and hDHFR. None of them was active against hDHFR. Only compound **28a** showed weak inhibitory activity against LmDHFR. Compound **4a** was selected for further development on the basis of synthetic feasibility and biological activity (IC<sub>50</sub> and K<sub>i</sub> against LmPTR1 of 5.6 mM and 436 μM, respectively). The derivatization of the hit at position 5 of the thiadiazole ring (Figure 2) was expected to increase the affinity and the specificity for PTR1 by introduction of fragments that lead to more complex and drug-like compounds.

**Library Design, Synthesis, and Testing.** A first set of derivatives of compound **4a** with substitutions at position 5 was designed with the aim of increasing the affinity toward LmPTR1, as well as exploring molecular diversity (Figure 2, Supporting Information Table 2-SI), thereby aiding optimization of the molecular properties for drug-likeness.<sup>15</sup> The calculated ternary complex of LmPTR1-NADPH-**4a** shows the ligand to be involved in stacking interactions with both the nicotinamide ring of the cofactor and the phenyl ring of

Scheme 1. Synthesis of Compounds in Library B



Phe113, and making hydrogen bonds with the diphosphate and the ribose moieties of NADPH and with the side chains of Ser111 and Tyr194. On the basis of this model, we derivatized position 5 because there is enough space to accommodate various different substituents. A variety of substituents were designed to introduce interactions with the residues lining this part of the binding site. Substituents encompass small aliphatic chains (**1b–3b**), one-ring aromatic systems with 0, 1, or 2 substituents (**4b–15b**), longer chains with a variable-size aliphatic bridge and one (**16b–23b**) or two (**24b–25b**) aromatic ring systems. All of these compounds comply with Lipinski's rule of five<sup>16</sup> (Supporting Information Table 2-SI). The compound library was obtained by reacting thiosemicarbazide with different carboxylic acids (Scheme 1) using Büchi's Syncore parallel synthesizer, resulting in 26 compounds, **1b–5b**, **7b–11b**, **13b–28b** (Supporting Information Table 3-SI). All designed compounds were obtained as [1,3,4]thiadiazol-2-ylamine with the appropriate substituent in the 5 position, except for compounds **6b** and **12b**, which were isolated only as the 5-substituted [1,3,4]-thiadiazol-2-ylamide of the corresponding acid: *N*-(5-pyridin-4-yl-[1,3,4]thiadiazol-2-yl)pyridine-4-carboxamide (**26b**) and *N*-[5-(3,4-dimethylphenyl)-[1,3,4]thiadiazol-2-yl]-3,4-dimethylbenzamide (**27b**). From the reactions of thiosemicarbazide with 3-chloropropionic acid or phthalimidoacetic acid were obtained both the [1,3,4]thiadiazol-2-ylamine derivative and 5-substituted [1,3,4]thiadiazol-2-ylamide, namely, **2b** (5-(2-chloroethyl)-[1,3,4]thiadiazol-2-ylamine) and **28b** (3-chloro-*N*-[5-(2-chloroethyl)-[1,3,4]thiadiazol-2-yl]-propionamide), **17b** (2-(5-amino-[1,3,4]thiadiazol-2-ylmethyl)-isoindole-1,3-dione), and **29b** (2-(1,3-dioxoisoindolin-2-yl)-*N*-5-(1,3-dioxoisoindolin-2-ylmethyl)-[1,3,4]thiadiazol-2-ylacetamide). Twenty-six

compounds were tested against LmPTR1 (Supporting Information Table 3-SI). Seven compounds (**7b**, **14b**, **15b**, **21b**, **22b**, **28b**, **29b**) showed competitive inhibition of LmPTR1 with respect to the dihydrofolate cofactor showing  $IC_{50}$  values between 22 and 309 mM corresponding to  $K_i$  values of 2–24 mM (Table 1, Figure 1). All these compounds were more active compared to the starting hit **4a** ( $IC_{50}$  5.6 mM) with the improvement in  $IC_{50}$  value being 254-fold in the case of the best compound, **15b**. The molecules were also tested for their activity against LmDHFR and hDHFR (Table 1, Figure 1). Only one compound, **21b**, showed an inhibitory activity against hDHFR with an  $IC_{50}$  value of 300  $\mu$ M. Two compounds, **15b** and **21b**, inhibited LmDHFR with  $IC_{50}$  values in the range 139–1300  $\mu$ M; thus, this class of derivatives showed specificity with respect to PTR1.

**Virtual Docking as a Basis for Lead Optimization.** Docking studies were performed on the tested compounds (**4a**, **1b**, **3b–5b**, **7b–11b**, **13b–29b**) with the aim of guiding the further synthetic elaboration of active compounds.

First, different crystal structures of LmPTR1 were retrieved from the Protein Data Bank<sup>17</sup> (Supporting Information Table 4-SI), and the docking procedure was tested by cross-docking all the ligands for which the crystal structures of their complexes with LmPTR1 were known. That is, for each of the seven crystal structures of LmPTR1-ligand complexes, the ligand was removed and the ligands from the other six crystal structures were docked into this protein structure and evaluated. Rmsd (root-mean-square deviation) values were calculated for the docking poses with respect to the ligand position in the crystal structures, either for all non-hydrogen atoms or for the core scaffold atoms. Fragments with high B-factors for the ligands 10-propargyl-5,8-dideazafolic

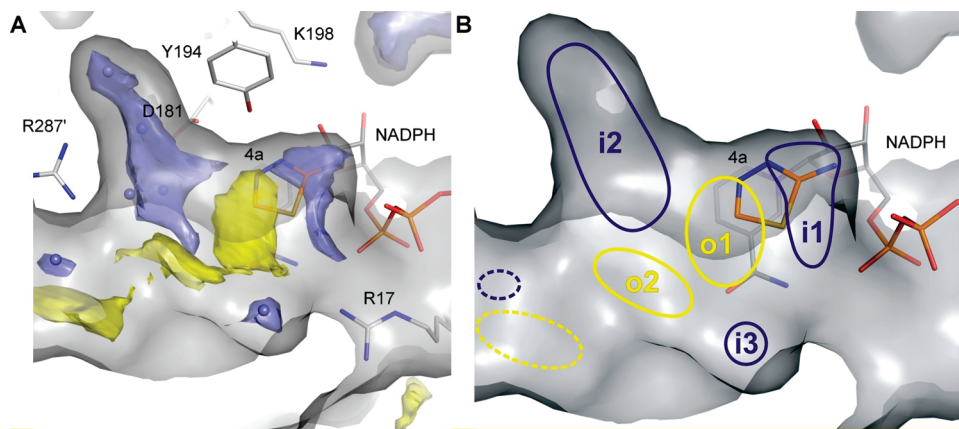


**Figure 3.** Interaction properties of the LmPTR1 active site. (A) The isosurfaces show energetically favorable regions for a hydrophilic water probe (blue,  $-6.0$  kcal/mol) and a hydrophobic “DRY” probe (yellow,  $-0.5$  kcal/mol) computed with the *GRID* program. The NADPH cofactor, docked [1,3,4]thiadiazole-2-amine compound, **4a**, and some important residues surrounding the active site are shown in stick representation. D181, Y194, and K198 are the catalytic triad residues involved in the first step of reduction. R287' is a residue from a second subunit of PTR1 which contributes to the hydrogen bond network of the water-filled pocket at the active site. Crystallographic water molecules are represented by blue spheres. The four water molecules close to R287' were treated explicitly for docking of ligands (see text for details). R17 and the nearby water molecule are important in the second step of the reduction reaction.<sup>26</sup> (B) Schematic representation of the main hydrophilic (blue) and hydrophobic (yellow) regions in the active site of PTR1 identified with the *GRID* calculations. The regions marked with dashed lines are somewhat further away from the active site and are not conserved among all the PTR1 structures investigated.

acid (CB3 of PDB ID: 2BFA) and **2** (methotrexate; 2-{4-[(2,4-diamino-pteridin-6-ylmethyl)-methyl-amino]-benzoyl-amino}-pentanedioic acid)<sup>18</sup> (MTX of PDB ID: 1E7W) (Supporting Information Figure 1-SI) were omitted. The initial results obtained using both the *GOLD* v 3.2<sup>19,20</sup> and *GLIDE*<sup>21</sup> programs were unsatisfactory with three of the ligands showing rmsd values over 5 Å for some or all of the target LmPTR1 structures. The poor docking poses could, however, be improved by including the four most conserved water molecules (with a conservation of 100%, 86%, 71%, and 71%, respectively, in the crystal structures used) in the binding site of LmPTR1 near the nicotinamide ring of the cofactor. These water molecules were identified by a cluster analysis based on all crystallographic water molecules in the listed crystal structures of LmPTR1. The use of these four conserved water molecules in combination with the *GOLD* program and the embedded GoldScore fitness function improved the cross-docking of the ligands to the different target structures. The average rmsd values of the 10 docking solutions for each ligand in the different receptor structures dropped below 2.2 Å for 5,6,7,8-tetrahydrobiopterin (THB of PDB ID: 2BF7) and below 1.2 Å for 7,8-dihydrobiopterin (HBI of PDB ID: 1E92 and 2BF7). The average RMSDs for 2,4,6-triaminoquinazoline (TAQ of PDB ID: 1W0C) and methotrexate (MTX of PDB ID: 1E7W) were higher and lay between 2.0 and 4.2 Å, respectively. Docking of 10-propargyl-5,8-dideazafoolic acid (CB3 of PDB ID: 2BFA) and trimethoprim (TOP of PDB ID: 2BFM) remained poor, showing an average rmsd between 2.7 and 7.0 Å.

After evaluating the docking procedure, 27 compounds (**4a**, **1b**, **3b–5b**, **7b–11b**, **13b–29b**) were docked into the LmPTR1 crystal structure (PDB ID: 1E92). The docking position for **4a** identified with *GOLD* was very similar to that found with LUDI during virtual screening, with the ring of the compound sandwiched between the side chain of Phe113 and the nicotinamide ring of the cofactor. On one hand, this result prompted us to use the calculate binding modes to design further synthetic elaborations of the active compounds by a structure-based approach. On the other hand, we wanted to check if the docking procedure could also

correctly rank the docked compounds. Therefore, we compared the *GOLD* scores and the inhibitory activity data for the docked compounds. The results showed that these scores could not discriminate between active and inactive compounds. A second trial was done by rescoring the calculate binding poses with *Autodock 4*.<sup>22</sup> The results showed that all but one active compound had a negative computed binding free energy, whereas the computed binding free energies of the inactive compounds were both positive and negative. This means that, in this second trial, we obtained many false positive results but only one false negative result. The positive energy values resulted from large Lennard-Jones energies due to van der Waals bumps. Energy minimization with *AMBER*<sup>23</sup> and computation of interaction energy terms did not, however, lead to better discrimination between active and inactive compounds. In summary, the docking calculations gave useful insights into the possible binding modes of the compounds, even though they had a limited predictive ability for activity.

Finally, docking of the same set of compounds was also performed against two crystal structures of hDHFR to get insights into the selectivity of these compounds. With a few exceptions, the thiadiazole ring did not dock on top of the nicotinamide ring of NADPH as observed for LmPTR1, but instead faced a hydrophilic pocket in the core of the active site. This suggests that the compounds would have different binding modes to the two enzymes and are good candidates for binding selectively to LmPTR1 and not to hDHFR.

**Structure-Based Comparative Analysis of LmPTR1 and hDHFR to Guide Further Lead Optimization.** In the context of the docking results and analysis of available X-ray structures of PTR1 and hDHFR, molecular interaction fields calculated with the *GRID* program<sup>24,25</sup> were used to suggest possible extensions of the original lead compound, **4a**. We focus our analysis and discussion on the LmPTR1 structure (PDB ID: 1E92). The *GRID* calculations were however performed for all available PTR1 structures listed in Table 4-SI of the Supporting Information.

The calculations showed several hydrophilic and hydrophobic regions in the active site of LmPTR1. The hydrophilic

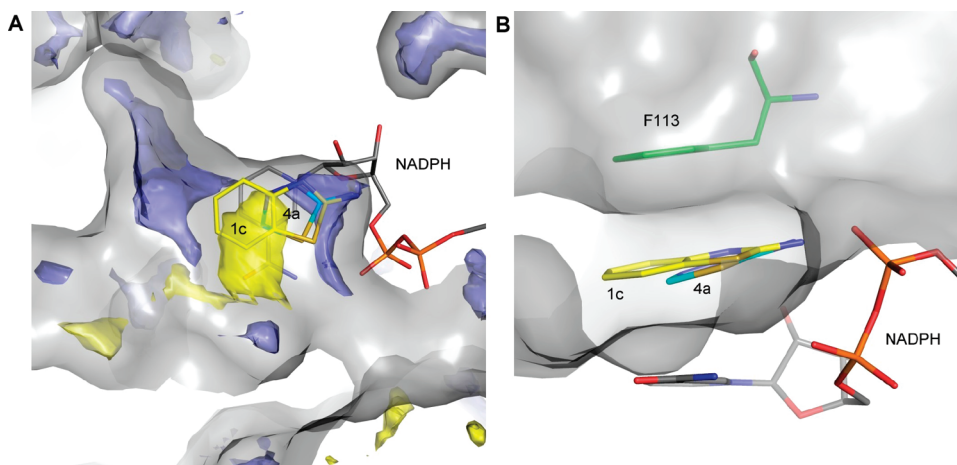


**Figure 4.** Docked configurations of [1,3,4]thiadiazole-2-ylamine, **4a**, (blue) and 1,3-benzothiazole-2-ylamine, **1c**, (yellow) at the active site of LmPTR1. (A) Top view. Hydrophobic and hydrophilic regions are shown as in Figure 3. (B) Side view. Note the stacking interaction between the nicotinamide ring of the cofactor (below) and the side chain of residue F113 (above).

pocket labeled *i1* is above the ribose ring of the NADPH cofactor (Figure 3). A group located in this region may be involved in hydrogen bonds with nearby serine residues and the ribose ring of NADPH in a similar way to that observed in the X-ray structure of PTR1 bound to a substrate.<sup>26</sup> The large hydrophilic pocket labeled *i2* protrudes into the core of the protein and contains four rather conserved water molecules. A small hydrophilic pocket *i3* is at the opposite side of the active site and contains one water molecule, which is suggested to be a proton source in the second step of the reduction reaction.<sup>27</sup> The hydrophobic region *o1* is at the core of the active site surrounded by the previously mentioned hydrophilic regions. The hydrophobic region labeled *o2* extends from the core of the active site outward toward the surface of the protein. Further identified regions marked with dashed lines in Figure 3B are at the side of the active site and not conserved among the analyzed X-ray structures of the PTR1.

To investigate which binding regions might be most important to exploit to obtain selective inhibitors, we analyzed the binding of inhibitor **2** in the context of the *GRID* maps. Inhibitor **2** binds to both PTR1 and hDHFR, but crystal structures show that its orientation differs in these two proteins. In both cases, the diaminopteridine ring of **2** is involved in stacking interactions between the nicotinamide ring of NADPH and the aromatic ring of the protein residue, whereas the rest of the molecule points out of the active site with two carboxy groups exposed to the solvent. *GRID* calculations for both the PTR1 and hDHFR structures show that the hydrophilic patch, corresponding to *i1*, at the core of the active site coincides with the location of the amino groups of **2** and that the hydrophobic patch corresponding to *o1* partially coincides with the second pteridine ring. In both cases, the benzene ring of **2** coincides with the hydrophobic patch corresponding to *o2* at the exit of the active site. However, hDHFR does not have a deep hydrophilic pocket like *i2* in PTR1. Therefore, an extension of the lead compound toward this hydrophilic pocket might enhance selectivity of the compounds toward PTR1. As seen from the docked position of **4a** in LmPTR1, the *i1* region is already occupied with the amino group and the nitrogen in position 4, which may be involved in hydrogen bonds; therefore, no modifications were suggested on this side of the compound. However, the other side of **4a** is only partially inserted into

the hydrophobic region *o1*, and there is enough space for extension with a hydrophobic group. Furthermore, this region is sandwiched between the nicotinamide ring of the cofactor at the bottom of the active site and the aromatic ring of the Phe113 side chain from above. Therefore, we suggested extension of **4a** by adding a benzene ring, resulting in the 1,3-benzothiazole-2-amine compound, **1c**. Subsequent docking of **1c** showed that the thiazole ring of **1c** was in essentially the same position as that of the docked **4a**. The benzene ring overlapped better with the *o1* hydrophobic region and showed stacking interactions with the nicotinamide ring of the cofactor and the Phe113 side chain (Figure 4). Taken together, these results suggest that the proposed 1,3-benzothiazole-2-amino compound should exploit the physicochemical properties of the core of the active site better. This was confirmed by in vitro experiments in which **1c** was found to have greater inhibitory activity than **4a**, with a  $K_i$  value of 143  $\mu\text{M}$  compared to 436  $\mu\text{M}$  for **4a** (Table 1).

Taking the 1,3-benzothiazole-2-amine, **1c**, as a second starting hit, we identified further extensions of compound **1c** to better utilize the hydrophobic region *o2* (Figure 3), and the hydrophilic pocket *i2*. From comparison of the *GRID* results for the hDHFR active site (not shown) and for the LmPTR1 active site, better specificity of the compound toward PTR1 relative to hDHFR could be gained through these extensions. We searched for commercially available compounds with a 1,3-benzothiazole-2-amine core and small substituents that might extend into these regions of the active site. Four compounds (**2c–5c**) were selected. Compound **5c** (6-trifluoromethoxybenzothiazol-2-ylamine) is also known as riluzole.<sup>28</sup>

**Testing of Benzothiazole Compounds.** Five benzothiazole compounds (**1c–5c**) were purchased and tested for their effect on the activity of LmPTR1, LmDHFR, and hDHFR (Table 1, Figure 1). All compounds inhibit LmPTR1 with  $\text{IC}_{50}$  values in the range from 40  $\mu\text{M}$  to 1.8 mM ( $K_i$  values from 3 to 143  $\mu\text{M}$ ). Only two of them (**2c** and **4c**) show a weak inhibition of LmDHFR activity (with  $\text{IC}_{50}$  values of 1.4 and 1.8 mM, respectively), whereas three compounds (**3c–5c**) inhibit hDHFR with  $\text{IC}_{50}$  values from 89  $\mu\text{M}$  to 1 mM. The best compounds, **3c** and **5c**, with  $\text{IC}_{50}$  values of 40 and 50  $\mu\text{M}$ , respectively, show a lower inhibitory activity against hDHFR ( $\text{IC}_{50}$  values of 89 and 312  $\mu\text{M}$ , respectively) and do not inhibit LmDHFR.

**Table 2.** Effect of Different Compounds, Administered at 50  $\mu\text{g/mL}$ , Alone or Combined with **1** at 30  $\mu\text{g/mL}$ , on the Growth of *Leishmania promastigotes*<sup>a</sup>

compound	growth of <i>L. mexicana</i> (%)	growth of <i>L. major</i> (%)	ED <sub>50</sub> of human MRC5 fibroblasts ( $\mu\text{g/mL}$ )
<b>1</b>	102.5 $\pm$ 0.3	68.0 $\pm$ 1.2	16.23 $\pm$ 2.47
<b>7b</b>	111.6 $\pm$ 0.7	105.6 $\pm$ 1.9	10% inhibition at 100 $\mu\text{g/mL}$
<b>7b + 1</b>	15.6 $\pm$ 0.5	38.0 $\pm$ 0.7	ND
<b>14b</b>	111.6 $\pm$ 1.4	83.5 $\pm$ 1.5	51.50 $\pm$ 5.52
<b>14b + 1</b>	18.2 $\pm$ 1.5	40.9 $\pm$ 0.2	ND
<b>15b</b>	131.9 $\pm$ 2.1	76.0 $\pm$ 1.4	43.03 $\pm$ 5.15
<b>15b + 1</b>	35.1 $\pm$ 10.9	14.6 $\pm$ 0.9	ND
<b>21b</b>	96.9 $\pm$ 0.7	85.1 $\pm$ 1.5	34.36 $\pm$ 3.72
<b>21b + 1</b>	27.3 $\pm$ 8.1	17.5 $\pm$ 0.2	ND
<b>28b</b>	4.7 $\pm$ 0.7	7.1 $\pm$ 0.2	4.18 $\pm$ 0.43
<b>28b + 1</b>	3.5 $\pm$ 0.2	4.1 $\pm$ 0.2	ND
<b>5c</b>	21.5 $\pm$ 0.7	101.8 $\pm$ 1.8	27.88 $\pm$ 3.17
<b>5c + 1</b>	15.1 $\pm$ 1.4	22.9 $\pm$ 0.004	ND

<sup>a</sup> ED<sub>50</sub> values vs human MRC5 fibroblast. Data are expressed as percentage of growth compared to control cultures to which no compound had been added. The results for *L. mexicana*, *L. major*, and human cells are given as the mean  $\pm$  SD from three independent experiments. ND = not detected.

**Testing the Compounds on Cultured Parasites.** Out of the six compounds (**7b**, **14b**, **15b**, **21b**, **28b**, **5c**) assayed on cultured promastigotes (insect stage) of *L. mexicana*, only **28b** and **5c** were able, as a single agent at 50  $\mu\text{g/mL}$ , to reduce parasite growth compared to the control (Table 2). They did so by 95.3% and 78.5%, respectively, (with corresponding ED<sub>50</sub> values of 10.1  $\mu\text{g/mL}$  and 30.8  $\mu\text{g/mL}$ ). None of the other compounds showed an inhibitory effect at concentrations up to 100  $\mu\text{g/mL}$ . With *L. major* promastigotes, **14b**, **15b**, and **21b** tested as single agents at 50  $\mu\text{g/mL}$  showed a moderate effect on parasite growth with a percentage of growth inhibition in the range 14.9–24.0%. Only **28b** showed strong inhibition with a percentage of growth inhibition above 90% (ED<sub>50</sub> 22.1  $\mu\text{g/mL}$ ) (Table 2). In parallel experiments, the ED<sub>50</sub> value for the control, the approved antileishmaniasis drug, Amphotericin B, was determined to be 0.1  $\mu\text{g/mL}$ .

All compounds were tested in combination with **1**, a known antifolate drug with a therapeutic indication for malaria that can be administered in combination with sulfadoxine (trade name *Fansidar*). It is not usually active against infections caused by trypanosomatids. When our new compounds were tested in combination with **1**, growth inhibition of both *L. major* and *L. mexicana* promastigotes was observed in all cases (Table 2, Figure 5). **1** alone, at 30  $\mu\text{g/mL}$ , showed no effect on growth of *L. mexicana* and reduced that of *L. major* by 32%. However, **1** in the presence of 50  $\mu\text{g/mL}$  of each of the other compounds caused considerable reduction of growth of the parasites. For *L. mexicana*, the percentage of growth compared to cells not treated with the compounds was between 15.6% (**7b** plus **1**) and 35.1% (**15b** plus **1**). For *L. major*, the remaining growth was between 14.6% (**15b** plus **1**) and 40.9% (**14b** plus **1**). At the measured concentration, all these compounds, except **28b** and **5c** which are active as a single agent, show a synergy with **1** against *L. mexicana* and against *L. major*.

The toxicity of the compounds was assayed on human MRC-5 cell line derived from fibroblasts. The ED<sub>50</sub> values are indicated in Table 2. Almost all compounds showed inhibition of growth of the MRC-5 cells at moderately toxic levels with ED<sub>50</sub> values ranging from 4  $\mu\text{g/mL}$  (**28b**) to 51  $\mu\text{g/mL}$  (**14b**). **1** and **5c** showed ED<sub>50</sub> values of 16  $\mu\text{g/mL}$  and 28  $\mu\text{g/mL}$ , respectively. As a positive exception, compound **7b** showed very little inhibition of growth of MRC-5 cells, thus indicating that this compound has low toxicity.

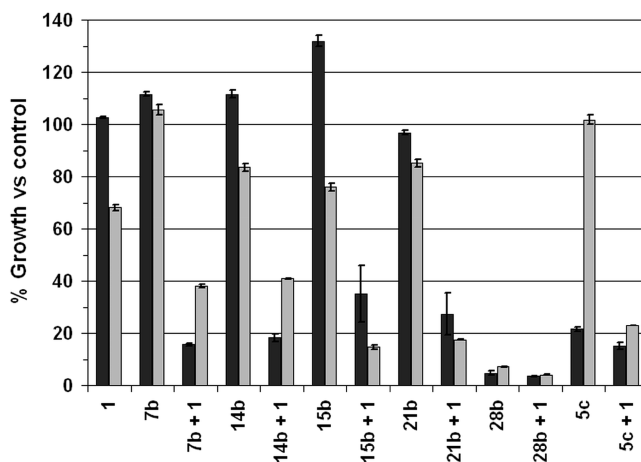


**Figure 5.** Growth of *L. mexicana* (in black) and *L. major* (in gray) parasites in the presence of 30  $\mu\text{g/mL}$  **1** and/or thiadiazole/benzothiazole compounds at a concentration of 50  $\mu\text{g/mL}$ . The growth values are expressed as percentages calculated with respect to the growth of parasites without **1** and thiadiazole/benzothiazole compounds.

### Concluding Discussion

From the three rounds of drug discovery involving computational and experimental approaches, we have identified 18 nonfolate compounds with specific inhibitory activity against LmPTR1. Some of them have been shown to inhibit the PTR1 protein at the low micromolar level (Table 1) and show specificity with respect to the human DHFR enzyme. Five compounds were found to be active in inhibiting parasite growth when administered in combination with **1**, a well-know DHFR inhibitor. The compounds show synergetic activity at the concentrations tested with the known DHFR inhibitor, **1**, indicating the value of inhibiting PTR1 and DHFR simultaneously in order to block folate reduction in *Leishmania* parasites. In particular, **7b** showed over 85% of parasite growth inhibition in combination with **1** and almost no toxicity against the MRC5 cells suggesting better safety profile with respect to the other compounds and **1** itself. Two compounds, **28b** and **5c**, have also been shown to be active when administered as single agents at 50  $\mu\text{g/mL}$ . Comparison of the toxicity and specificity profiles suggests that several of the compounds identified in these screens, including **28b** and **5c**, provide a useful basis for further studies to discover clinical agents against leishmaniasis and possibly other parasitic diseases.

Interestingly, **5c** is a known clinical drug, riluzole, which is used to treat amyotrophic lateral sclerosis with moderate toxicity. It has also been proposed for the treatment of mood and anxiety disorders, probably as glutamate receptor modulator.<sup>27</sup>

We searched in DrugBank (www.drugbank.ca) for other benzothiazole derivatives or benzothiazole containing drugs and found that there is only one drug currently in use: Ethoxazolamide (DrugBank code: DB00311, PubChem CID: 3295). It is a carbonic anhydrase inhibitor used as a diuretic and in glaucoma. These findings suggest that benzothiazole compounds are drug-like molecules and prospective chemical modulation of the decorating fragments could improve their specificity as antiparasitic drugs and improve their safety profile.

Independently, Mpamhanga et al.<sup>12</sup> have, by employing different computational and medicinal chemistry approaches, identified similar compounds, containing the aminobenzothiazole scaffold, as inhibitors of *Trypanosoma brucei* PTR1.

Encouragingly, their crystal structures of 2-aminobenzimidazole and 1-(3,4-dichloro-benzyl)-2-amino-benzimidazole in complex with *T. brucei* PTR1 show the ligand in a similar orientation in the binding site to that which we found in our docking studies for similar compounds. We have conducted crystallization trials for LmPTR1 with inhibitors identified in this work (not shown), but we were unable to obtain any suitable crystals of protein–inhibitor complexes. However, unlike the compounds identified in ref 12, our compounds show promising inhibitory activity in parasite promastigotes.

In conclusion, the compounds designed and tested here in combination with **1** have potential for therapeutic application against important neglected diseases.

## Materials and Methods

**Virtual Screening.** The structure of LmPTR1 (PDB ID: 1E92) was considered for the virtual screening. The bound cofactor NADP<sup>+</sup> in its oxidized form was replaced by NADPH in the reduced form, taken from the LmPTR1 complex (PDB ID: 1EW7). All water molecules and other ligands were removed and not considered during the calculation. *WHATIF*<sup>29</sup> and *AMBER 8.0*<sup>23</sup> were used to add missing hydrogen atoms. LUDI<sup>14</sup> was used within the *InsightII*<sup>30</sup> suite of programs to perform the virtual screening of the ACD database (~350 000 molecules) against the LmPTR1 three-dimensional structural model. The parameters used were as follows: Energy-Estimate-3 as scoring function, 10 Å as the radius and the centroid of the bound natural substrate, dihydrobiopterin, as the center of the sphere used to screen the molecules. The 21 394 results so obtained were filtered based on three parameters computed for each screened ligand: contact percentage (> 50); number of H bonds (> 1); calculated score (> 400). The calculated poses of the resultant 724 ligands were visually analyzed. The analyzed ligands were grouped based on the number and type of interactions established and the residues with which they interact. Molecules that were predicted to form a stacking interaction with Phe113 and H bonds with active site residues were selected preferentially. Visual comparison of the structures of the active sites of LmPTR1 and hDHFR was used to prioritize the predicted interactions to obtain more specific compounds. Following this selection, 53 molecules were suggested for enzymatic screening.

**Preparation of Protein Crystal Structures.** The X-ray crystal structures of the PTR1 and hDHFR proteins were downloaded from the PDB;<sup>17</sup> see Supporting Information Table 4-SI for a complete list of the structures used in this study. The PTR1 protein is a homotetramer; thus, the subunit labeled chain A was

extracted from all PTR1 structures and aligned on chain A of the structure 1E92 using the *Chimera*<sup>31</sup> program. Residue Arg287 from chain D was also included because it is located close to the active site of chain A. Water molecules and ions were removed, hydrogens were added, and all structures were minimized using the Maestro modeling environment.<sup>21</sup>

**Structural Analysis and Comparison.** The *GRID* program<sup>24,25</sup> was used to determine energetically favorable binding sites for different chemical groups in the region of the active site of the PTR1 and hDHFR proteins in the presence of cofactor. A set of probes representing hydrophobic and hydrophilic chemical groups with hydrogen bond donor or acceptor properties were used for the calculations. The grid spacing was set to 0.5 Å and other parameters were assigned default values.

**Docking Procedures.** The *GOLD v 3.2*<sup>19,20</sup> and *GLIDE*<sup>21</sup> programs were used for ligand docking. For *GOLD*, two fitness functions, GoldScore and ChemScore,<sup>32</sup> were used, and proteins and ligands were input in Mol2 format. The binding site was defined as being within a sphere of radius of 20 Å from the hydroxyl O atom of Tyr194. The number of output docking solutions was set to 10, and the other parameters were set to default values. For GoldScore, tests were done allowing two bumps between the ligand and the protein during docking. For *GLIDE*, receptor grids were centered on the centroid of Tyr194. Docking was performed with standard precision (SP), with the options “dock flexibly” and “allow flips of 5 and 6 member rings” enabled. Output was set to 10 poses per ligand after post-docking minimization. The other parameters were set as default. For cross-docking tests, the ligand structures were taken from the crystal structures of LmPTR1. For docking other compounds, the three-dimensional structures of the molecules were built and energy minimized using Maestro<sup>21</sup> or Corina.<sup>33</sup> The compounds were protonated using Epik.<sup>21</sup> The compounds were docked into the LmPTR1 structure with PDB ID: 1E92 (chain A plus Arg287 of chain D). Compounds were also docked into two structures of hDHFR (PDB ID: 1KMS and 1U72) with NADPH bound to aid in assessment of binding selectivity.

The WatCH<sup>34</sup> program was used for the cluster analysis of the crystallographic water sites in the superimposed LmPTR1 crystal structures with a threshold of 2.4 Å. To include the water molecules in selected *GOLD* docking runs, two water sites were set as “on” and two sites were set to “toggle”. During the docking, *GOLD* could automatically determine whether these specific waters were bound or not. The orientation of the waters was optimized by *GOLD* with the option “spin”.

Tests of rescoring of the best pose found by *GOLD* were performed by computing the free energy of binding of the complex using *AutoDock 4.0*<sup>22</sup> with the parameter “epdb”. This binding free energy includes the ligand intramolecular contributions as well as intermolecular electrostatic and desolvation contributions. Rescoring with the *AMBER* force field<sup>35</sup> was also tested. 100 steps of steepest descent energy minimization of the docked structures was performed with Amber8 using the *AMBER* ff03 forcefield. The cofactor and protein atoms, except hydrogens, were restrained using a harmonic force constant of 10 kcal/mol/Å<sup>2</sup> and the following parameter settings: imin = 1, maxcyc = 100, ntmn = 1, ncyc = 100, nsnb = 20, igb = 0, ntb = 0, dielc = 1.0, ntpr = 10, ntr = 1, cut = 15.0, eedmeth = 5. The Lennard-Jones and Coulombic contributions to the interaction energy were then computed using ptraj.

**Synthetic Chemistry.** The reagents were purchased from Sigma-Aldrich. Reactions were performed using Büchi's Syn-core parallel synthesizer. Reaction progress was monitored by TLC on precoated silica gel 60 F<sub>254</sub> plates (Merck) and visualization was accomplished with UV light (254 nm). Yields of these reactions referred to purified products were in the range 30–45%. Compounds **7b**, **14b**, **15b**, and **21b** were resynthesized through microwave synthesis to obtain a larger amount for growth inhibition tests with cultured parasites. Small-scale open-vessel microwave reactions were conducted using a commercially



available single-mode microwave unit (CEM Discover). The machine consists of a continuously focused microwave power delivery system with operator selectable power output from 0 to 300 W. Reactions were performed in a 50 mL round-bottom flask. The temperature of the contents of the vessel was monitored using an IR sensor located underneath the reaction vessel. The contents of the vessel were stirred by means of a rotating magnetic plate located below the floor of the microwave cavity and a Teflon-coated magnetic stir bar in the flask. Temperature and power profiles were monitored using commercially available software provided by the microwave manufacturer. Yields of these reactions referred to purified products were in the range 55–70%. Purification by flash column chromatography was conducted using Sigma-Aldrich SilicaGel (grade 9385, pore size of 60 Å, 230–400 mesh). Purity of all compounds was determined to be at least 95% from TLC and elemental analyses. This analysis was performed on a Perkin-Elmer 240C instrument, and the results for C, H, and N were within  $\pm 0.4\%$  of theoretical values. The synthesized compounds were characterized by  $^1\text{H}$  NMR on a Bruker FT-NMR AVANCE 400. Spectra were recorded in DMSO- $d_6$ . Chemical shifts are reported as  $\delta$  values (ppm) referenced to tetramethylsilane as an internal standard. When peak multiplicities are given, the following abbreviations are used: s, singlet; d, doublet; t, triplet; q, quartet; m, multiplet; dd double doublet; dt double triplet; dq double quartet; br, broadened signal.

**General Procedure for the in-Parallel Synthesis.** To an ice-cooled mixture of thiosemicarbazide (0.150 g, 1.65 mmol) and the corresponding carboxylic acid (1.65 mmol), an excess of phosphorus oxychloride (0.3 mL, 3.3 mmol) was added slowly and under continuous stirring. Subsequently, the temperature was raised gradually to 75–80 °C. The reaction was kept at this temperature and stirred for 3 h. Ice–water was added, and the mixture was stirred for an additional hour and the solvent removed by filtration under reduced pressure. The residual precipitate was suspended in water and 7 mL of 20% sodium bicarbonate solution was added to remove the unreacted carboxylic acid. Afterward, the mixture was filtrated under vacuum and the obtained solid was treated with an acidic or basic solution to remove the starting material. For compounds **2b**, **7b**, **14b**, **15b**, and **17b**, chromatography purification ( $\text{CH}_2\text{Cl}_2/\text{MeOH}$  9:1) was performed. The obtained solid was dried in vacuo.

**General Procedure for the Microwave Synthesis.** To an ice-cooled mixture of thiosemicarbazide (0.30 g, 3.3 mmol) and the corresponding carboxylic acid (2.2 mmol), an excess of phosphorus oxychloride (0.6 mL, 6.6 mmol) was added slowly and under continuous stirring. The flask was placed in the microwave cavity. Microwave irradiation of 50 W was used, the temperature being ramped from room temperature to 75 °C. Once 75 °C was reached, the reaction mixture was held at this temperature for 10 min. The glue was allowed to cool to room temperature and manually stirred; the microwave irradiation was repeated. Ice–water was added and the mixture was stirred for an hour. NaOH (3 M) was added to the mixture until pH 11 was reached. The volume was reduced under vacuum, and the mixture of products isolated by filtration was purified and separated by chromatography column ( $\text{CH}_2\text{Cl}_2/\text{MeOH}$  9:1).

**3-(5-Amino-[1,3,4]thiadiazol-2-yl)-pyridin-4-ylamine (7b).**  $^1\text{H}$  NMR  $\delta$  8.28 (s, 1H), 7.97 (d,  $J = 5.7$  Hz, 1H), 7.4 (br, 4H), 6.72 (d,  $J = 5.7$  Hz, 1H). Elemental analysis: calcd for  $\text{C}_7\text{H}_7\text{N}_5\text{S}$ , C, 43.51; H, 3.65; N, 36.24. Found: C, 43.50; H, 3.65; N, 36.25.

**5-(1H-benzo[d][1,2,3]triazol-5-yl)-[1,3,4]thiadiazol-2-ylamine (14b).**  $^1\text{H}$  NMR  $\delta$  8.20 (s, 1H), 7.99 (d,  $J = 8.8$  Hz, 1H), 7.93 (d,  $J = 8.7$  Hz, 1H), 7.47 (br, 2H). Elemental analysis: calcd for  $\text{C}_8\text{H}_6\text{N}_6\text{S}$ , C, 44.03; H, 2.77; N, 38.51. Found: C, 44.17; H, 2.77; N, 38.49.

**2-(5-Amino-[1,3,4]thiadiazol-2-yl)-4H-chromen-4-one (15b).**  $^1\text{H}$  NMR  $\delta$  7.90 (d,  $J = 8.2$  Hz, 1H), 7.75 (d,  $J = 7.8$  Hz, 1H), 7.50 (t,  $J = 7.8$  Hz, 1H), 7.49 (dd,  $J = 8.2, 7.8$  Hz, 1H), 6.93

(s, 1H). Elemental analysis: calcd for  $\text{C}_{11}\text{H}_7\text{N}_3\text{O}_2\text{S}$ , C, 53.87; H, 2.88; N, 17.13. Found: C, 53.69; H, 2.88; N, 17.11.

**3-(5-Amino-[1,3,4]thiadiazol-2-yl)-1-(thiophen-2-yl)propan-1-one (21b).**  $^1\text{H}$  NMR  $\delta$  7.90 (dd,  $J = 3.8, 1.1$  Hz, 1H), 7.83 (dd,  $J = 5.0, 1.1$  Hz, 1H), 7.20 (t,  $J = 3.8$  Hz, 1H), 3.45 (dt,  $J = 8.2, 1.2$  Hz, 2H), 3.00 (dt,  $J = 7.0, 0.4$  Hz, 2H). Elemental analysis: calcd for  $\text{C}_9\text{H}_9\text{N}_3\text{OS}_2$ , C, 45.17; H, 3.79; N, 17.56. Found: C, 45.18; H, 3.79; N, 17.55.

**3-(5-Amino-[1,3,4]thiadiazol-2-yl)-1-(4-chlorophenyl)propan-1-one (22b).**  $^1\text{H}$  NMR  $\delta$  7.99 (d,  $J = 8.8$  Hz, 2H), 7.60 (d,  $J = 8.8$  Hz, 2H), 3.24 (t,  $J = 6.3$  Hz, 2H), 2.57 (t,  $J = 6.3$  Hz, 2H). Elemental analysis: calcd for  $\text{C}_{11}\text{H}_{10}\text{ClN}_3\text{OS}$ , C, 49.35; H, 3.76; N, 15.69. Found: C, 49.40; H, 3.75; N, 15.65.

**3-Chloro-N-[5-(2-chloroethyl)-[1,3,4]thiadiazol-2-yl]propionamide (28b).**  $^1\text{H}$  NMR  $\delta$  4.01 (t,  $J = 6.5$  Hz, 2H), 3.92 (t,  $J = 6.5$  Hz, 2H), 3.48 (t,  $J = 6.5$  Hz, 2H), 3.00 (t,  $J = 6.5$  Hz, 2H). Elemental analysis: calcd for  $\text{C}_7\text{H}_9\text{Cl}_2\text{N}_3\text{OS}$ , C, 33.08; H, 3.57; N, 16.53. Found: C, 33.34; H, 3.70; N, 16.69.

**2-(1,3-Dioxoisindolin-2-yl)-N-5-(1,3-dioxoisindolin-2-ylmethyl)-[1,3,4]thiadiazol-2-ylacetamide (29b).**  $^1\text{H}$  NMR  $\delta$  8.0–7.8 (m, 8H), 5.14 (s, 2H), 4.60 (s, 2H). Elemental analysis: calcd for  $\text{C}_{21}\text{H}_{13}\text{N}_5\text{O}_5\text{S}$ , C, 56.37; H, 2.93; N, 15.65. Found: C, 54.38; H, 2.93; N, 15.68.

**Enzymology.** Proteins were purified as described.<sup>36–44</sup> Folate cofactors and substrates were a gift from Eprova; all other substrates, cofactors, and reagents were purchased from different companies at the maximum purity grade. Compounds **1a–53a** and **1c–5c** and **1** were purchased from different vendors and purity of key compounds evaluated to be higher than 95% (the elemental analysis is reported in Supporting Information). For determination of reductase activity, NADPH oxidation was followed at 340 nm.<sup>45</sup>  $K_m$  values were determined by measuring the dependence of the enzyme activity on substrate concentration using folic acid as the substrate. The  $K_m$  value was 2.5  $\mu\text{M}$  for LmPTR1. Kinetic measurements with DHFR were performed at 25 °C in standard enzyme buffer.<sup>46</sup>  $K_m$  values were determined by measuring the dependence of the enzyme activity on substrate concentration using dihydrofolate as the substrate. The  $K_m$  values of dihydrofolate for hDHFR and LmDHFR in this buffer were determined to be 7  $\mu\text{M}$  and 3.5  $\mu\text{M}$ , respectively. The kinetic experiments were carried out in triplicate, and no individual measurement differed by > 20% from the mean.

All tested compounds (**1a–53a**, **1b**, **3b–5b**, **7b–11b**, **13b–29b**, **1c–5c**) were dissolved in DMSO. Compounds **1a–53a** were initially screened for inhibitory activity against LmPTR1 at a single concentration (500  $\mu\text{M}$ ). Compounds **1b**, **3b–5b**, **7b–11b**, and **13b–29b** were initially screened for inhibition of LmPTR1 activity at a single concentration (5  $\mu\text{M}$ ). For those compounds which were found to be active against LmPTR1, a complete set of measurements was performed to determine the  $\text{IC}_{50}$  values. For compounds **1c–5c**, the  $\text{IC}_{50}$  value against LmPTR1 was obtained.  $K_i$  values were obtained from  $\text{IC}_{50}$  plots by assuming competitive inhibition.<sup>47,48</sup> For compound **15b**, the  $K_i$  value was determined by Lineweaver–Burk analysis of multiple substrate and inhibitor concentrations and showed a competitive inhibition pattern with respect to the dihydrofolate cofactor. The result was consistent with the value determined from the  $\text{IC}_{50}$  plots (data not shown).

Compounds **4a**, **6a**, **28a**, **35a**, **38a**, **53a**, **7b**, **14b**, **15b**, **21b**, **22b**, **28b**, **29b**, **1c–5c** were screened for their activity against LmDHFR and hDHFR. The compounds were screened at a single concentration in the range of 25  $\mu\text{M}$  to 1 mM. For those compounds which were found to be active, an  $\text{IC}_{50}$  value was estimated by considering a linear relation between the percentage of inhibition and concentration.

No incubation effect was detected for any compound. All compounds discussed here behaved well kinetically and do not fall into the category of aggregation-based promiscuous inhibitors.<sup>49</sup> The DMSO concentration was kept below the concentration affecting enzyme activity (1% for PTR1).

**Biological Evaluation.** Parasitology. Promastigote forms of *L. mexicana* (MHOM/BZ/84/BEL46) and *L. major* (MHOM/SU/73/5-ASKH) were cultured in SDM-79 medium, pH 7.3, supplemented with 15% heat-inactivated fetal calf serum, penicillin (100 units/mL), and streptomycin (100 mg/mL) at 28 °C under water-saturated air with 5% CO<sub>2</sub> as described earlier.<sup>50</sup> The cultures were initiated at 10<sup>5</sup> parasites/mL, and cells were harvested at a density of 2 × 10<sup>7</sup> parasites/mL.

To estimate the concentrations at which compounds cause 50% inhibition of growth (effective dose, ED<sub>50</sub>) of cultured *Leishmania* promastigotes, the Alamar Blue micromethod, based on monitoring the reducing environment of proliferating cells, was used as previously described.<sup>51</sup> Briefly, cultures were diluted in medium to 1 × 10<sup>6</sup> parasites/mL and seeded in 96-well flat-bottom microplates (Nunc) to a final volume of 100 μL. Inhibitor stock solutions were in DMSO. For each compound, dilutions were made in culture medium and added to the parasite cultures giving a series of concentrations starting from 100 μg/mL downward. The final DMSO concentration in the cultures was always less than 1%. Each inhibitor concentration was tested in duplicate. Controls with DMSO alone in the medium (which never caused any growth inhibition at the concentration used) and the parasites without compounds were also tested. After 72 h of incubation at 28 °C, 10 μL Alamar Blue was added to each well, and after 4 h incubation at 28 °C, its fluorescence was quantified at an excitation wavelength of 530 nm and at an emission wavelength of 590 nm. ED<sub>50</sub> values were calculated by linear interpolation. The optical density in the absence of drugs was set as the 100% control. Assays with the commercial antileishmaniasis drug, Amphotericin B, were also carried out in order to have reference values. Three independent experiments, each in duplicate, were performed for the determination of the ED<sub>50</sub> value of each compound.

In separate experiments, compounds were tested in combination with **1** to evaluate the synergic effect. Combinations were tested with each compound at a single dose of 50 μg/mL and **1** at 30 μg/mL, in duplicate. The percentage of growth inhibition of promastigotes in the presence of the combination of each compound with **1** was compared with controls in which only the compound was added at 50 μg/mL and with controls without the compound and **1**.

**Toxicity Test.** The fibroblast cell line MRC-5 was used to determine the possible toxicity of compounds for human cells. The fibroblasts were grown in DMEM medium (Gibco) supplemented with 10% heat-inactivated FBS and extra glutamine, at 37 °C in humidified incubators in an atmosphere of 5% CO<sub>2</sub>. The assay was performed using essentially the same method as used for parasites. To each well of the microplates, without or with compound at different concentrations, cells were added at a density such that, after 72 h of incubation, adhesive cells have formed a confluent monocellular film in control wells. Alamar Blue was added to each well after 72 h and used to determine cell growth, similarly to that described above for parasites.

**Acknowledgment.** We gratefully acknowledge support of the Italian Internationalization Programme (2006–2008) and Cassa di Risparmio di Modena Internationalization Programme (Kinetodrugs project, 2008–2010) and the Klaus Tschira Foundation. We are grateful to the “Centro Interdipartimentale Grandi Strumenti” of the University of Modena and Reggio Emilia and to the “Fondazione Cassa di Risparmio di Modena” for supplying the NMR spectrometer. We thank Prof. L. Brasili for allowing us to use the single mode microwave unit, and Merck-Eprova-AG (www.eprova.com) for supplying of folate cofactors and substrates.

**Supporting Information Available:** Table 1-SI, Compounds **1a–53a** and their enzyme inhibition activity; Table 2-SI, Compounds **1b–25b** and their molecular properties; Table 3-SI,

Compounds **1b**, **3b–5b**, **7b–11b**, **13b–29b** and their enzyme inhibition activity; Table 4-SI, Protein structures used in this study; Elemental analysis of the key compounds **4a**, **6a**, **28a**, **35a**, **38a**, **53a**, **1c–5c**, and **1**, and characterization of **1b–5b**, **8b–13b**, **16b–20b**, **23b–27b**. This material is available free of charge via the Internet at <http://pubs.acs.org>.

## References

- (1) Sundar, S.; Makharia, A.; More, D. K.; Agrawal, G.; Voss, A.; Fischer, C.; Bachmann, P.; Murray, H. W. Short-course of oral miltefosine for treatment of visceral leishmaniasis. *Clin. Infect. Dis.* **2000**, *31*, 1110–1113.
- (2) Then, R. L. Antimicrobial dihydrofolate reductase inhibitors--achievements and future options: review. *J. Chemother.* **2004**, *16*, 3–12.
- (3) McGuire, J. J. Anticancer antifolates: current status and future directions. *Curr. Pharm. Des.* **2003**, *9*, 2593–2613.
- (4) Gregson, A.; Plowe, C. V. Mechanisms of resistance of malaria parasites to antifolates. *Pharmacol. Rev.* **2005**, *57*, 117–145.
- (5) Nare, B.; Hardy, L. W.; Beverley, S. M. The roles of pteridine reductase 1 and dihydrofolate reductase-thymidylate synthase in pteridine metabolism in the protozoan parasite *Leishmania major*. *J. Biol. Chem.* **1997**, *272*, 13883–13891.
- (6) Senkovich, O.; Pal, B.; Schormann, N.; Chattopadhyay, D. Trypanosoma cruzi genome encodes a pteridine reductase 2 protein. *Mol. Biochem. Parasitol.* **2003**, *127*, 89–92.
- (7) Cunningham, M. L.; Titus, R. G.; Turco, S. J.; Beverley, S. M. Regulation of differentiation to the infective stage of the protozoan parasite *Leishmania major* by tetrahydrobiopterin. *Science* **2001**, *292*, 285–287.
- (8) Nare, B.; Luba, J.; Hardy, L. W.; Beverley, S. New approaches to *Leishmania* chemotherapy: pteridine reductase 1 (PTR1) as a target and modulator of antifolate sensitivity. *Parasitology* **1997**, *114* Suppl, S101–S110.
- (9) Bello, A. R.; Nare, B.; Freedman, D.; Hardy, L.; Beverley, S. M. PTR1: a reductase mediating salvage of oxidized pteridines and methotrexate resistance in the protozoan parasite *Leishmania major*. *Proc. Natl. Acad. Sci. U.S.A.* **1994**, *91*, 11442–11446.
- (10) Cavazzuti, A.; Paglietti, G.; Hunter, W. N.; Gamarro, F.; Piras, S.; Loriga, M.; Allecca, S.; Corona, P.; McLuskey, K.; Tulloch, L.; Gibellini, F.; Ferrari, S.; Costi, M. P. Discovery of potent pteridine reductase inhibitors to guide antiparasite drug development. *Proc. Natl. Acad. Sci. U.S.A.* **2008**, *105*, 1448–1453.
- (11) Tulloch, L. B.; Martini, V. P.; Iulek, J.; Huggan, J. K.; Lee, J. H.; Gibson, C. L.; Smith, T. K.; Suckling, C. J.; Hunter, W. N. Structure-based design of pteridine reductase inhibitors targeting african sleeping sickness and the leishmaniasis. *J. Med. Chem.* **2010**, *53*, 221–229.
- (12) Mpamhanga, C. P.; Spinks, D.; Tulloch, L. B.; Shanks, E. J.; Robinson, D. A.; Collie, I. T.; Fairlamb, A. H.; Wyatt, P. G.; Frearson, J. A.; Hunter, W. N.; Gilbert, I. H.; Brenk, R. One scaffold, three binding modes: novel and selective pteridine reductase 1 inhibitors derived from fragment hits discovery by virtual screening. *J. Med. Chem.* **2009**, *52*, 4454–4465.
- (13) Russell, P.; Hitching, G. Aryl derivatives of 2,4-diaminopyrimidines. *J. Am. Chem. Soc.* **1951**, *73*, 3763–3770.
- (14) Boehm, H. J. The computer program LUDI: a new method for the de novo design of enzyme inhibitors. *J. Comput.-Aided. Mol. Des.* **1992**, *6*, 61–78.
- (15) Mishra, H.; Singh, N.; Lahiri, T.; Misra, K. A comparative study on the molecular descriptors for predicting drug-likeness of small molecules. *Bioinformation* **2009**, *3*, 384–388.
- (16) Lipinski, C. A.; Lombardo, F.; Dominy, B. W.; Feeney, P. J. Experimental and computational approaches to estimate solubility and permeability in drug discovery and development settings. *Adv. Drug Delivery Rev.* **2001**, *46*, 3–26.
- (17) www.pdb.org.
- (18) Seeger, D.; Cosulich, O.; Smith, J., Jr.; Hultquist, M. 4-Amino derivatives of pteroylglutamic acid. *J. Am. Chem. Soc.* **1949**, *71*, 1753–1758.
- (19) Jones, G.; Willett, P.; Glen, R. C. Molecular recognition of receptor sites using a genetic algorithm with a description of desolvation. *J. Mol. Biol.* **1995**, *245*, 43–53.
- (20) Jones, G.; Willett, P.; Glen, R. C.; Leach, A. R.; Taylor, R. Development and validation of a genetic algorithm for flexible docking. *J. Mol. Biol.* **1997**, *267*, 727–748.
- (21) *Maestro*, *Glide* (version 4.5), and *Epik*, Schrödinger, LLC, New York, NY, 2008.
- (22) Morris, G. M.; Huey, R.; Lindstrom, W.; Sanner, M. F.; Belew, R. K.; Goodsell, D. S.; Olson, A. J. AutoDock4 and AutoDockTools4:

- automated docking with selective receptor flexibility. *J. Comput. Chem.* **2009**, *30*, 2785–2791.
- (23) Case, D. A.; Cheatham, T. E., III; Darden, T.; Gohlke, H.; Luo, R.; Merz, K. M., Jr.; Onufriev, A.; Simmerling, C.; Wang, B.; Woods, R. J. The Amber biomolecular simulation programs. *J. Comput. Chem.* **2005**, *26*, 1668–1688.
- (24) Goodford, P. J. A computational procedure for determining energetically favorable binding sites on biologically important macromolecules. *J. Med. Chem.* **1985**, *28*, 849–857.
- (25) Molecular Discovery; <http://www.moldiscovery.com/>
- (26) Gourley, D. G.; Schuttelkopf, A. W.; Leonard, G. A.; Luba, J.; Hardy, L. W.; Beverley, S. M.; Hunter, W. N. Pteridine reductase mechanism correlates pterin metabolism with drug resistance in trypanosomatid parasites. *Nat. Struct. Biol.* **2001**, *8*, 521–525.
- (27) Arun, P.; Moffett, J. R.; Nambodiri, A. M. A. Riluzole decrease synthesis of N-Acetylaspartate and N-acetylaspartylglutamate in SH-SY5Y human neuroblastoma cells. *Brain Res.* **2010**, *1334*, 25–30.
- (28) Jimonet, P.; Audiau, F.; Barreau, M.; Blanchard, J.-C.; Boireau, A.; Bour, Y.; Coléno, M.-A.; Doble, A.; Doerflinger, G.; Do Huu, C.; Donat, M.-H.; Duchesne, J. M.; Ganil, P.; Guérémy, C.; Honoré, E.; Just, B.; Kerphirique, R.; Gontier, S.; Hubert, P.; Laduron, P. M.; Le Blevec, J.; Meunier, M.; Miquet, J.-M.; Nemecek, C.; Pasquet, M.; Piot, O.; Pratt, J.; Rataud, J.; Reibaud, M.; Stutzmann, J.-M.; Mignani, S. *J. Med. Chem.* **1999**, *42*, 2828–2843.
- (29) Vriend, G. WHAT IF: a molecular modeling and drug design program. *J. Mol. Graph.* **1990**, *8*, 52–56.
- (30) Insight II. (2000). Molecular Simulations Inc., San Diego, CA. Accelrys.
- (31) Pettersen, E. F.; Goddard, T. D.; Huang, C. C.; Couch, G. S.; Greenblatt, D. M.; Meng, E. C.; Ferrin, T. E. UCSF Chimera—a visualization system for exploratory research and analysis. *J. Comput. Chem.* **2004**, *25*, 1605–1612. <http://www.cgl.ucsf.edu/chimera>.
- (32) Eldridge, M. D.; Murray, C. W.; Auton, T. R.; Paolini, G. V.; Mee, R. P. Empirical scoring functions. I. the development of a fast empirical scoring function to estimate the binding affinity of ligands in receptor complexes. *J. Comput.-Aided Mol. Des.* **1997**, *11*, 425–445.
- (33) Sadowski, J.; Rudolph, C.; Gasteiger, J. Automatic generation of 3D atomic coordinates for organic molecules. *Tetrahedron Comput. Methodol.* **1990**, *3*, 537–547.
- (34) Sanschagrin, P. C.; Kuhn, L. A. Cluster analysis of consensus water sites in thrombin and trypsin shows conservation between serine proteases and contributions to ligand specificity. *Protein Sci.* **1998**, *7*, 2054–2064.
- (35) Duan, Y.; Wu, C.; Chowdhury, S.; Lee, M. C.; Xiong, G.; Zhang, W.; Yang, R.; Cieplak, P.; Luo, R.; Lee, T.; Caldwell, J.; Wang, J.; Kollman, P. A point-charge force field for molecular mechanics simulations of proteins based on condensed-phase quantum mechanical calculations. *J. Comput. Chem.* **2003**, *24*, 1999–2012.
- (36) Dann, J. G.; Ostler, G.; Bjur, R. A.; King, R. W.; Scudder, P.; Turner, P. C.; Roberts, G. C.; Burgen, A. S. Large scale purification and characterization of dihydrofolate reductase from a methotrexate-resistant strain of *Lactobacillus casei*. *Biochem. J.* **1976**, *157*, 559–571.
- (37) Hanahan, D. Studies on transformation of *Escherichia coli* with plasmids. *J. Mol. Biol.* **1983**, *166*, 557–580.
- (38) Meek, T. D.; Garvey, E. P.; Santi, D. V. Purification and characterization of the bifunctional thymidylate synthetase-dihydrofolate reductase from methotrexate-resistant *Leishmania tropica*. *Biochemistry* **1985**, *24*, 678–686.
- (39) Maley, G. F.; Maley, F. Properties of a defined mutant of *Escherichia coli* thymidylate synthase. *J. Biol. Chem.* **1988**, *263*, 7620–7627.
- (40) Santi, D. V.; Edman, U.; Minkin, S.; Greene, P. J. Purification and characterization of recombinant *Pneumocystis carinii* thymidylate synthase. *Protein Expr. Purif.* **1991**, *2*, 350–354.
- (41) Livi, L. L.; Edman, U.; Schneider, G. P.; Greene, P. J.; Santi, D. V. Cloning, expression and characterization of thymidylate synthase from *Cryptococcus neoformans*. *Gene* **1994**, *150*, 221–226.
- (42) Pedersen Lane, J.; Maley, G. F.; Chu, E.; Maley, F. High level expression of human thymidylate synthase. *Protein Expr. Purif.* **1997**, *10*, 256–262.
- (43) Robello, C.; Navarro, P.; Castanys, S.; Gamarro, F. A pteridine reductase gene ptr1 contiguous to a P-glycoprotein confers resistance to antifolates in *Trypanosoma cruzi*. *Mol. Biochem. Parasitol.* **1997**, *90*, 525–535.
- (44) Gourley, D. G.; Luba, J.; Hardy, L. W.; Beverley, S. M.; Hunter, W. N. Crystallization of recombinant *Leishmania major* pteridine reductase 1 (PTR1). *Acta Crystallogr., Sect. D* **1999**, 1608–1610.
- (45) Bello, A. R.; Nare, B.; Freedman, D.; Hardy, L.; Beverley, S. M. PTR1: a reductase mediating salvage of oxidized pteridines and methotrexate resistance in the protozoan parasite *Leishmania major*. *Proc. Natl. Acad. Sci. U.S.A.* **1994**, *91*, 11442–11446.
- (46) Tan, X. H.; Huang, S. M.; Ratnam, M.; Thompson, P. D.; Freisheim, J. H. The importance of loop region residues 40–46 in human dihydrofolate reductase as revealed by site-directed mutagenesis. *J. Biol. Chem.* **1990**, *265*, 8027–8032.
- (47) Chou, T. Relationships between inhibition constants and fractional inhibition in enzyme-catalyzed reactions with different numbers of reactants, different reaction mechanisms, and different types and mechanisms of inhibition. *Mol. Pharmacol.* **1974**, *10*, 235–247.
- (48) Segel, I. H. *Enzyme Kinetics: Behaviour and Analysis of Rapid Equilibrium and Steady-State Enzyme Systems*; Wiley: New York, 1975.
- (49) McGovern, S. L.; Caselli, E.; Grigorieff, N.; Shoichet, B. K. A common mechanism underlying promiscuous inhibitors from virtual and high-throughput screening. *J. Med. Chem.* **2002**, *45*, 1712–1722.
- (50) Brun, R.; Schönenberger, M. Cultivation and in vitro cloning or procyclic culture forms of *Trypanosoma brucei* in a semi-defined medium. *Acta Trop.* **1979**, *36*, 289–292.
- (51) Mikus, J.; Steverding, D. A simple colorimetric method to screen drug cytotoxicity against *Leishmania* using the dye Alamar Blue. *Parasitol. Int.* **2000**, *48*, 265–269.